784. Combustion variability and uniqueness in cylinders of a large power radial engine

Michal Gęca[1], Miroslaw Wendeker[2], Grzegorz Litak[3]
[1, 2]Department of Thermodynamics, Fluid Mechanics and Aircraft Propulsion
Lublin University of Technology, Nadbystrzycka 36, PL-20-618 Lublin, Poland
[3]Department of Applied Mechanics
Lublin University of Technology, Nadbystrzycka 36, PL-20-618 Lublin, Poland
E-mail: [1]*m.geca@pollub.pl*, [2]*m.wendeker@pollub.pl*, [3]*g.litak@pollub.pl*
Phone: +4881 538 4573, **fax:** +4881 538 4233.

Abstract. This paper analyzes variability and uniqueness of a combustion process in the spark ignition radial engine having nine cylinders. In the case of single cylinder disturbances, multifractal approach is proposed to identify faults in the measured cylinder pressure. For better clarity, the pressure cyclic response is illustrated by means of wavelet results. The examined engine was powered by an electronic fuel injection, giving the possibility of varying doses supplied to the individual cylinders.

Keywords: spark ignition engine dynamics, cycle-to-cycle pressure oscillations, wavelets, non-linear vibrations.

Introduction

Radial piston engines were used in aviation from its early beginning. Despite extensive development of jet and turbine engines they are still competitive (low cost of purchase and maintenance). Radial piston engines have also a favorable power-to-weight ratio. This article considers the world's largest stellar engine. The power unit has been manufactured in Poland for over 70 years and originally is powered by carbureted system. The main problems of these engines include the imbalanced work of cylinders. Research conducted by the American company Radial Engines, Ltd., which manufactures seven cylinder R755B2 Jacobs radial engines (275 hp), show that power generated in each cylinder is different [1]. This effect is due to the thermodynamic state of the uniqueness of the combustion process reflected by cycle to cycle combustion variation and structural factors. Various sources of cylinder pressure oscillations for spark ignition engines were initially identified and classified by Heywood [2]. Furthermore, the construction of an air cooled piston engine leads to different temperature distribution on the surface of the cylinder strokes. In a radial engine, the cylinders are located around the crankshaft and all pistons are connected by a common crank-piston mechanism. Consequently, the crankshaft consists of a main shaft, and the side rods. This construction leads to the differentiation of the stroke, where the individual cylinders show slightly different degree of compression and cylinder capacity. Each cylinder can exhibit particular cycle to cycle variability of the combustion process. The uniqueness of each cylinder affects the non-uniformity of the entire engine. The way to reduce the non-uniformity of the engine was to replace the power supply carburetor by an electronic fuel injection system. The injectors located in the individual intake pipes of cylinders provide individually dosed fuel to each cylinder. Thus, the control system is sharing fuel delivery to differently distributed cylinders.

Analyzing the pressure response in the individual cylinders is the most efficient way of identifying a combustion process [3-6]. The cycle-by-cycle variations in heat release in a spark ignition internal combustion engine were analyzed by means of a low dimension numerical simulations and simplified turbulent combustion models [7-10]. It's worth noticing that traditional techniques of time series analysis based on Fourier transform can distinguish periodic trends in engine cylinders in a frequency domain. However they cannot capture occurrences of

extreme events, intermittency and other non-stationarities which could arise in a disturbed cylinder signal. These can be studied by following the ups and downs of the amplitude in a time domain. Thus, for internal combustion engines, the use of multifractal analysis (MA) [11-12] and simultaneous time-frequency studies by a continuous wavelet transform (CWT) [13-14] become useful tools. Mono-fractal and multifractal approaches were used to characterize the fluctuations for several air-fuel ratio values, φ from lean mixtures to stoichiometric situations in engine from both experimental data [4, 15-16] and simulated from combustion model [10]. This method has shown its advantages to estimate the set of critical exponents, especially from singular and turbulent signal data telling about the properties of a combustion process, particularly about its complexity and correlations.

On the other hand, wavelets are very useful to identify non-stationarities and intermittences of a combustion process [4, 9, 15-17]. In the present paper we apply such approaches to diagnose 9-cylinder radial aircraft engine.

Engine parameters are specified in Table 1, while the operating range with the measuring point - in Fig. 1a. Fig. 1b gives its photo. Below, we focus on the identification of a faulty operation of a cylinder among the other ones.

Table 1. ASz62IR engine specification

Item	Value
Engine type	Four stroke, SI, air-cooled
Number of cylinder	9
Cylinder arrangement	Single star
Bore, stroke	155,5 mm × 174,5 mm
Displacement volume	29,87 dm^3
Compression ratio	6,4 : 1
Power	860 kW – 2200 rpm
Specific fuel consumption	235 kg/h
Charging	Mechanical – max pressure 0,133 MPa
Ignition type	Double-spark magneto
Fuel system	Multipoint Electronic Injection

Experimental Procedure

The present test covers the engine operation in steady state defined by the rotational velocity and load expressed as the pressure in the intake manifold (Fig. 1a) while average air-fuel ratio was chosen as $\lambda = 0.7$ at each cylinder.

The measurements have been performed for the average rotational velocity of $n = 1770$ rpm and the engine load (0.094 MPa) between the propeller characteristics and the full power characteristics (Fig. 1a). At the measuring point the engine generates the power of 480 kW, and fuel consumption equals 109 kg/h. The fuel composition was obtained due to the injection time $t_1 = 7.8$ ms. Note that one of the cylinders was fuelled in a varying step way by alternating the injection time every 10 s from $t_1 = 7.8$ ms to $t_2 = 5.84$ ms according to the diagram in Fig. 2.

The tests were performed in the engine test laboratory at the constant temperature of 30 ºC and atmospheric pressure equal to 1005 hPa. The analysis deals with the range of over 950 subsequent operating cycles. The discrepancy in the number of analyzed cycles results from the research method that consists in maintaining the engine at a selected operating point for a 1 minute span which follows the necessity to obtain at least 900 subsequent cycles. Pressure measurement was performed with a sampling rate of 20 kHz. For each of cycle we estimated the indicated mean effective pressure (*IMEP*), defined as a constant alternative pressure which acts on the piston during the whole expansion stroke performs the same amount of work as the real variable pressure in the cylinder [2].
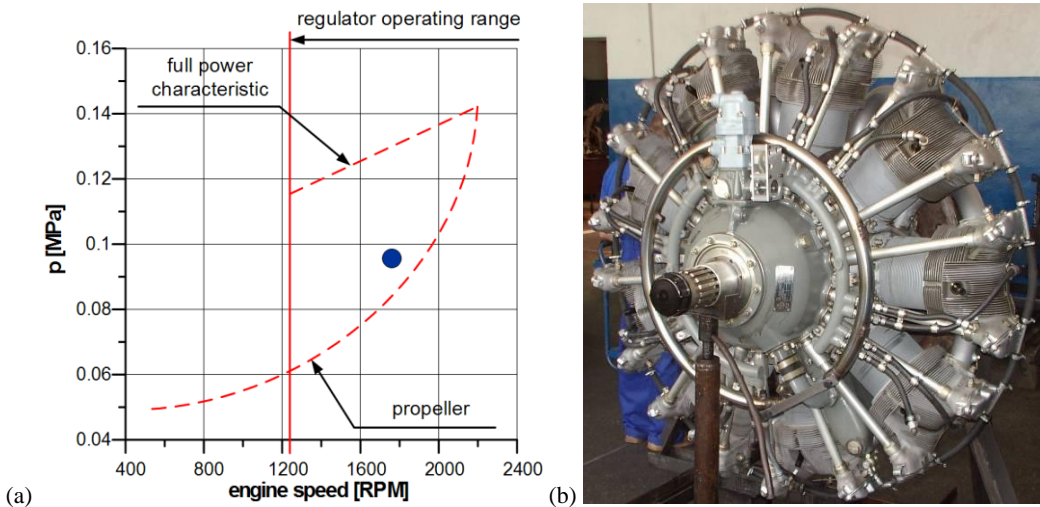
Fig. 1. Engine operating range and measuring point (a), photo of the examined engine (b)
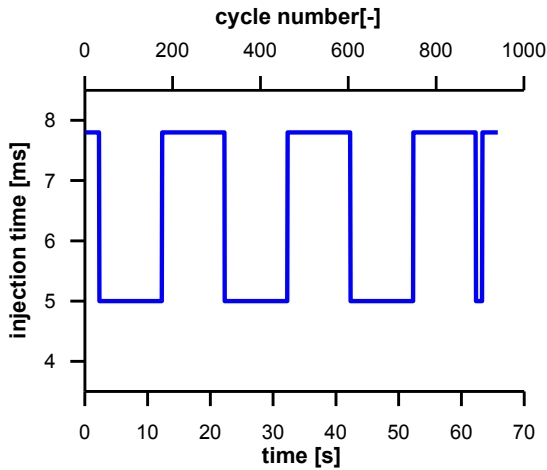

Fig. 2. Injection variation of mixture composition in the chosen single cylinder

Consequently, the cyclic *IMEP* can be expressed as:

$$IMEP(i) = \frac{L_i}{V_s},$$

(1)

where L_i is the work indicated in the cylinder at the combustion cycle i, and V_s is the piston displacement volume in the cylinder.

Fig. 3 illustrates the cyclic *IMEP*, where the cyclic work L_i was estimated numerically by integration of the measured pressure during air-fuel ratio variations by time dependent injection time (as shown in Fig. 2) in the chosen three cylinders 3, 5, 7. Visible differences in *IMEP* for various cylinders are influenced not only by the injection time disturbances in the specified cylinder but also by the individual differences of piston-cylinder systems, and their geometrical configuration (Fig. 1b).
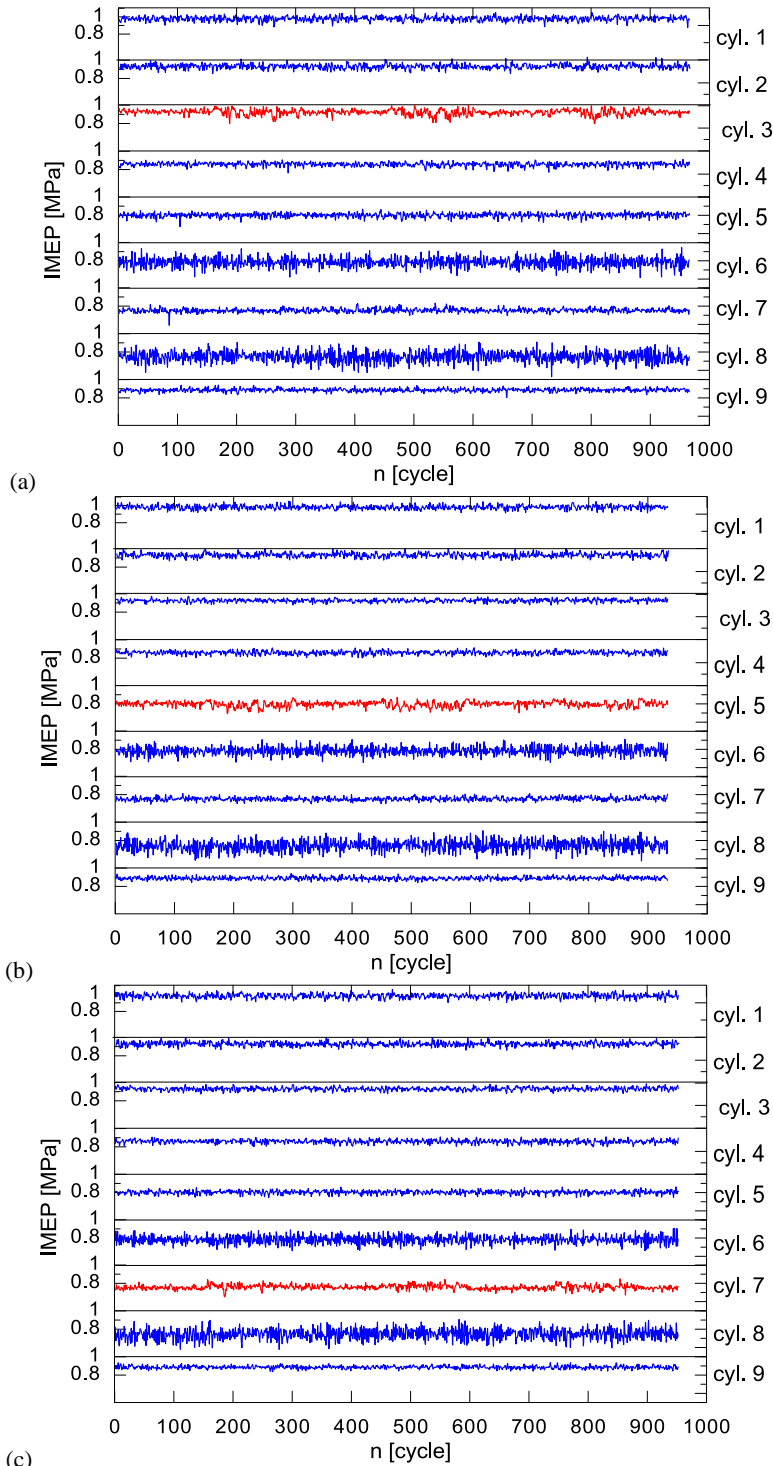
584

Fig. 3. Cyclic variations of *IMEP* measured simultaneously for all 9 cylinders during the disturbing amount of fuel (see Fig. 2) in the cylinder (a) 3, (b) 5, (c) 7 (marked in red). The remaining cylinders powered by a mixture composition of $\lambda = 0.7$

Multifractal Analysis

The three representative collections of *IMEP* time series presented in Fig. 3 were studied further using MA [10-12]. The spectrum of critical exponents is characterized by the most probable exponent α_0 telling about the correlation of the examined time series. This parameter, similarly to Hurst exponent, shows how persistent is the examined stochastic process. If $\alpha_0 < 0.5$ the process is anti–persistent (negatively correlated) while for $\alpha_0 > 0.5$ it is persistent (positively correlated). The two cases $\alpha_0 = 0.0$ and $\alpha_0 = 0.5$ correspond to a Gaussian random process characterized by the series of random numbers and Brownian random walk characterized by random steps, respectively.

Furthermore, the parameter $\Delta\alpha = \alpha_{max} - \alpha_{min}$, measuring the width of exponents distribution indicates the complexity in the time response. Each critical exponent α can be associated with the so-called Hölder exponent and estimated from the time series (Fig. 3) at each time instant (cycle) i_0:

$$| IMEP(i) - P_n(i - i_0) | \le C | i - i_0 |^{\alpha}, \tag{2}$$

where $P_n(i)$ is a polynomial of degree n less than α, and C is a constant. For the complex systems the exponent distribution forms a continuous band. Such an exponent band of one selected time series (cylinder 5 from case 1) is presented in Fig. 4. The estimated exponent distribution $f(\alpha)$ (see red points) was obtained by multifractal analysis. Then it was interpolated out by the 4th degree polynomial trend line described grade 4 (blue line) using the method of least squares.
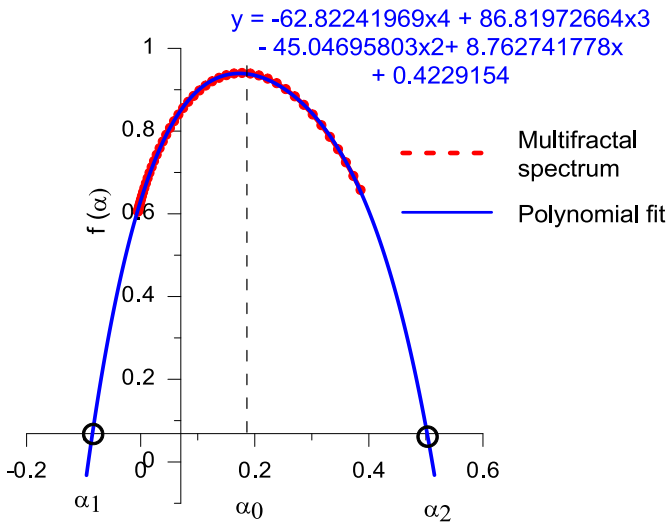

$$y = -62.82241969x^4 + 86.81972664x^3 - 45.04695803x^2 + 8.762741778x + 0.4229154$$

Fig. 4. Schematic strategy for determining the coefficients for the multifractal spectrum of the sample pressure time series in cylinder 5 (for the case 1 in Fig. 3a)

The above procedure (Eq. 2) has been applied to all time series in Fig. 2 including those of disturbed dose of fuel (see cylinder 3, 5 and 7 in Fig. 2a-c, respectively). For each test case the most expected exponent α_0 as well as range of critical exponents $\Delta\alpha$ were found. The results, presented in Fig. 5 indicate that the abnormal cylinder (with disturbed fuel composition) can be distinguished by the largest value $\alpha_0 \approx 0.3$ indicating the smallest negative correlation. On the other hand $\Delta\alpha$ is changing about 0.94 for the disturbed cylinder No. 3, 0.66 for the cylinder No.

586

5, and $\Delta\alpha = 0.89$ for the cylinder No. 7. Thus, in two cases the associated with the disturbed cylinder time series exhibit a relatively high complexity in comparison to other cases (time series in other cylinders).

Comparing the MF results in Fig. 5a, b, c, and d, which present the distribution of MF in the presence (Fig. 5a-c) and absence (Fig. 5d) of disturbances one can observe the points beyond the maximum value of $\Delta\alpha \approx 0.7$ and $\alpha_0 \approx 0.18$ (see Fig. 5d for absence of disturbances). In the case of disturbances of a single cylinder, the combustion process interferes by the crankshaft with other cylinders. After more systematic studies we noticed that this effect was not observed for cylinder 6 and 8. This could be related to different sensitivity of various cylinders, which are characterized by their unique locations.

Wavelet Analysis

For better clarity we study the disturbed *IMEP* time series given by CWT [13, 14]. The corresponding wavelet transform with respect to a wavelet function $\psi(\cdot)$ is defined as follows:

$$W_{s,n}(IMEP) = \sum_{i=1}^{N} \frac{1}{s}\psi\left(\frac{i-n}{s}\right)\frac{(IMEP(i)- <IMEP>)}{\sigma_{MIP}},$$ (3)

where $<IMEP>$ and σ_{IMEP} are the averages and standard deviations. The wavelet $\psi(t)$ is referred to as the mother wavelet, and the letters s and n denote the scale and the time index, respectively.

The wavelet power spectrum (WPS) of the *IMEP* time series is defined as the square modulus of the CWT:

$$P_W(s,n) = \left|W_{s,n}\right|^2.$$ (4)

In our calculations, we have used a complex Morlet wavelet as the mother wavelet. A Morlet wavelet consists of a plane wave modulated by a Gaussian function and is described by:

$$\psi(\eta) = \pi^{-1/4}e^{i\theta_0\eta}e^{-\eta^2/2},$$ (5)

where θ_0 is the center frequency, also referred to as the order of the wavelet.

The value of θ_0 defines the number of oscillations in the wavelet and thus controls the time/frequency resolutions. In our analysis, we used $\theta_0 = 6$. This choice provides a good balance between the time and frequency resolutions. Also, for this choice, the scale is approximately equal to the period, and therefore the terms scale and period can be interchanged for interpreting the results. The reader is referred to general discussion [13-14] and also to applications in combustion engines [5, 15-17] for further details on the wavelet analysis methodology. Fig. 6a-Fig. 6c provide the results of the CWT. Note that the modulation in fuel mixture composition (Fig. 2) forces the intermittent behavior [15]. Interestingly, the combustion variations appear in different time scales simultaneously. This effect is presumably caused by nonlinear factors [7].

Concluding Remarks

This study demonstrated that the maximum value of MF parameters for the case of abnormally working cylinder, simulated by variation of fuel injection time, can be identified by

multifractal analysis. Additionally, non-stationary work in cylinders is shown in wavelet power spectrum. Namely, Figs. 6a-c reveal the intermittent changes in pressure in the two domains simultaneously - in the time domain and frequency (or the respective periods) domain. Such behavior was forced by the periodically changing fuel composition.
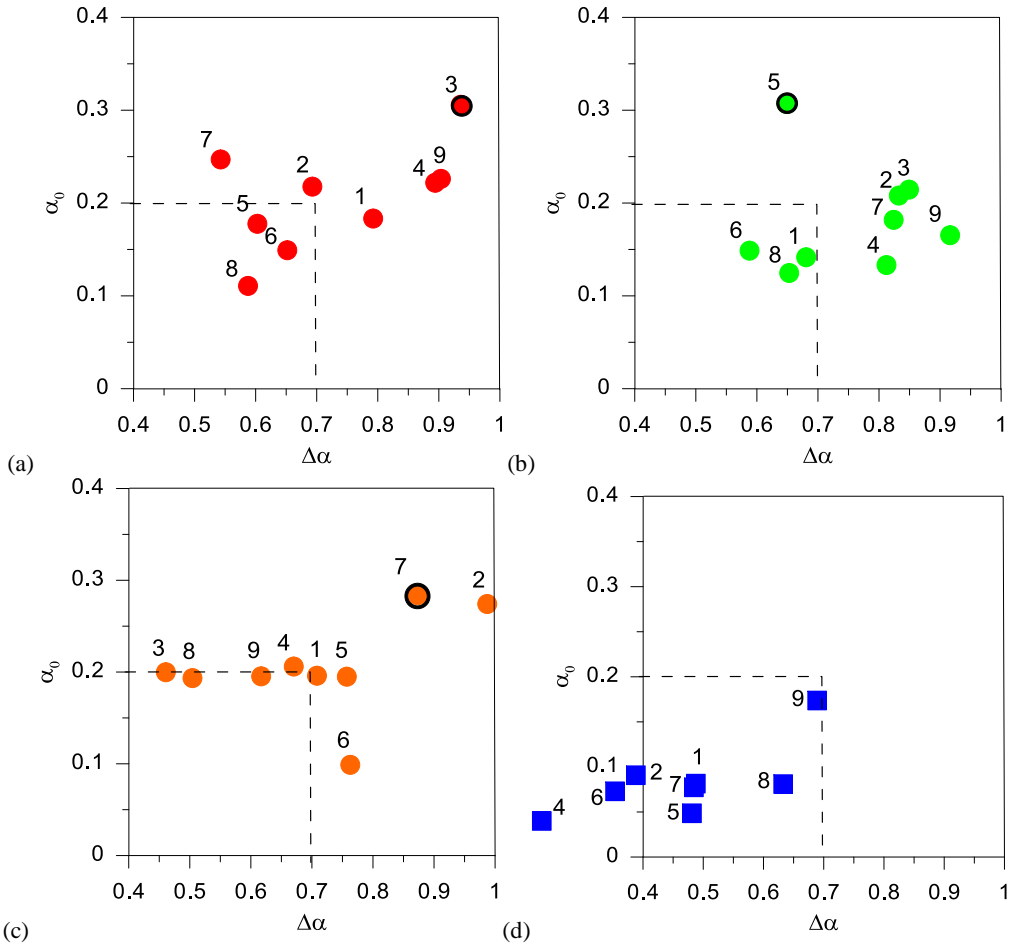

Fig. 5. Multifractal analysis of *IMEP*. Cylinders Nos. 3, 5, 7 were fed by varying the composition of the mixture (black border), the remaining cylinders powered by a mixture composition $\lambda = 0.7$ (a, b, c respectively). All cylinders powered by the constant mixture composition $\lambda = 0.7$ (d)

Our analysis indicates that various cylinders are sensitive to disturbances occurring in neighboring regions in different ways. That dependence on particular cylinder comes from the system geometry and working conditions. The presented results could be helpful in tracing the interaction between the processes of combustion in different cylinders, and consequently in developing recommendations for the implementation of a novel fuel injection strategy.
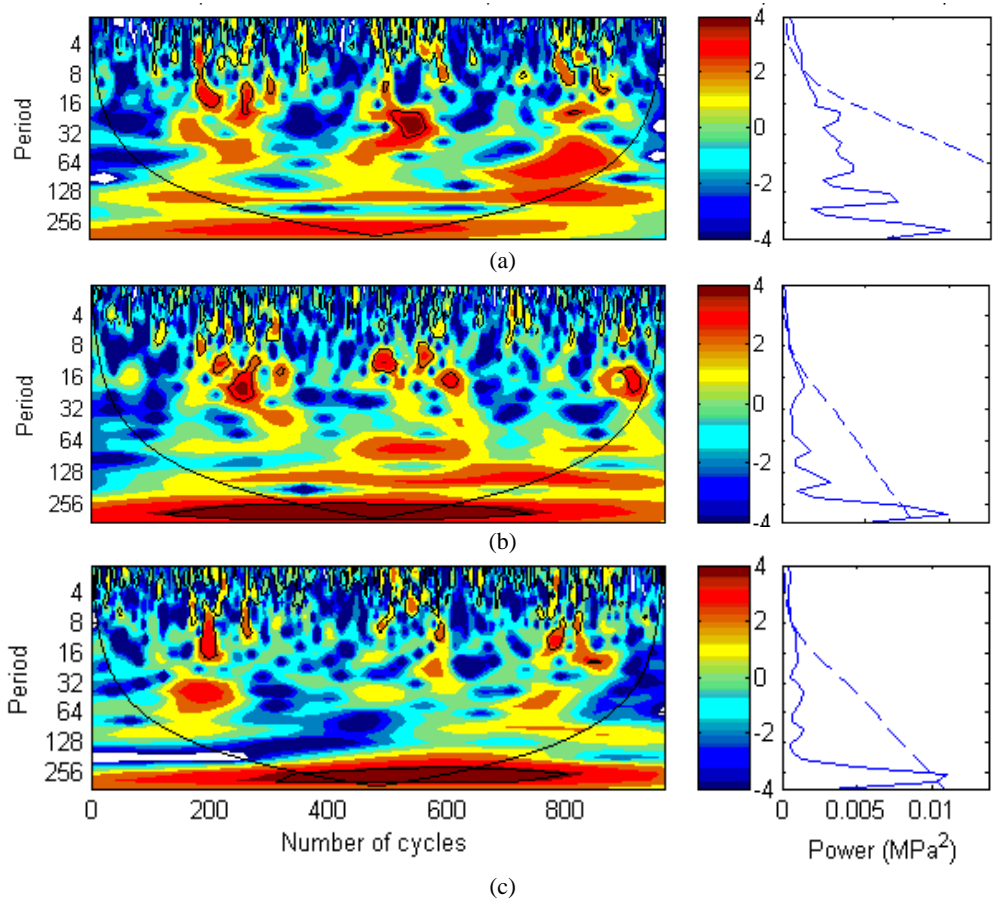
Acknowledgements

588

(a)

(b)

(c)

Fig. 6. Wavelet power spectra of *IMEP* estimate from measured pressure in cylinders with a disturbed mixture composition (Nos. 3, 5, 7 for (a), (b), and (c), respectively) with fuel injection time varying as presented in Fig. 2. The remaining cylinders powered by a mixture composition fixed to constant $\lambda = 0.7$

References

[1]   **Curry S.** Fuel Injecting the Jacobs Engines, www.radialengines.com, (visited 10.01.2012).
[2]   **Heywood J. B.** Internal Combustion Engine Fundamentals. New York: McGraw - Hill, 1988.
[3]   **Litak G., Kamiński T., Czarnigowski J., Sen A. K., Wendeker M.** Combustion process in a spark ignition engine: analysis of cyclic maximum pressure and peak pressure angle**.** Mechanika, Vol. 44, 2009, p. 1-11.
[4]   **Litak G., Geca M., Yao B.-F., Li G.-X.** Indicated mean effective pressure oscillations in a natural gas combustion engine. Zeitschrift fuer Naturforschung, 64A, 2009, p. 393-398.
[5]   **Longwic R., Sen A. K., Górski K., Lotko W., Litak G.** Cycle-to-cycle variations of the combustion process in a Diesel engine powered by different fuels. Journal of Vibroengineering, Vol. 13, 2011, p. 120-127.
[6]   **Hu Z.** Nonlinear instabilities of combustion processes and cycle-to-cycle variations in spark-ignition engines. SAE, 1996, Paper No. 961197.
[7]   **Daw C. S., Kennel M. B., Finney C. E. A., Connolly F. T.** Observing and modeling dynamics in an internal combustion engine. Phys. Rev. E, 57, 1998, p. 2811-2819.
[8]   **Daw C. S., Finney C. E. A., Tracy E. R.** A review of symbolic analysis of experimental data. Rev. Sci. Instrum., 74, 2003, p. 915-930.

[9] **Curto-Risso P. L., Medina A., Hernández A. C., Guzmán-Vargas L., Angulo-Brown F. L.** On cycle-to-cycle heat release variations in a simulated spark ignition heat engine. Applied Energy, 88, 2011, p. 1557-1567.

[10] **Curto-Risso P. L., Medina A., Hernández A. C., Guzmán-Vargas L., Angulo-Brown F. L.** Monofractal and multifractal analysis of simulated heat release fluctuations in a spark ignition heat engine. Physica A, 389, 2010, p. 5662-5670.

[11] **Muzy J. F., Bacry E., Arneodo A.** Wavelets and multifractal formalism for singular signals - application to turbulence data. Phys. Rev. Lett., 67, 1991, p. 3515-3518.

[12] **Goldberger A. L., Amaral L. A. N., Glass L., Hausdorff J. M., Ivanov P. Ch., Mark R. G., Mietus J. E., Moody G. B., Peng C.-K., Stanley H. E.** PhysioBank, physioToolkit, and physioNet components of a new research resource for complex physiologic signals. Circulation 101, 2000, p. E215 and the software provided on the webpage http://www.physionet.org/physiotools/multifractal/ (visited 20.12. 2011).

[13] **Torrence C., Compo G. P.** A practical guide to wavelet analysis. Bull. Amer. Meteor. Soc., 79, 1998, p. 61-78.

[14] **Kumar P., Foufoula-Georgiou E.** Wavelet analysis for geophysical applications. Rev. Geophys., 35, 1997, p. 385-412.

[15] **Sen A. K., Litak G., Finney C. E. A., Daw C. S., Wagner R. M.** Analysis of heat release dynamics in an internal combustion engine using multifractals and wavelets. Applied Energy, 87, 2010, p. 1736-1743.

[16] **Sen A. K., Litak G., Yao B.-F., Li G.-X.** Regular and intermittent pressure oscillations in a natural gas-fired internal combustion engine. Appl. Therm. Eng., 30, 2010, p. 776-779.

[17] **Tily R., Brace C. J.** Analysis of cyclic variability in combustion in internal combustion engines using wavelets. Proc. Inst. Mech. Engin., Part D: J. Autom. Engin., 225, 2011, p. 341-353.